Catalysis Science & Technology

Identifying hydroxylated copper dimers in SSZ-13 via UV-vis spectroscopy

Journal:	*Catalysis Science & Technology*
Manuscript ID	CY-COM-02-2022-000353.R1
Article Type:	Communication
Date Submitted by the Author:	06-Apr-2022
Complete List of Authors:	Göltl, Florian; The University of Arizona Bhandari, Saurabh; University of Wisconsin Madison, Chemical and Biological Engineering Lebron-Rodriguez, Edgard; University of Wisconsin Madison, Chemical and Biological Engineering Gold, Jake; University of Wisconsin Madison, Chemical and Biological Engineering Zones, Stacey; Chevron Energy Technology Co, Catalysts Hermans, Ive; University of Wisconsin-Madison, Chemistry; University of Wisconsin-Madison, Chemical and Biological Engineering Dumesic, James; University of Wisconsin Madison, Chemical and Biological Engineering Mavrikakis, Manos; University of Wisconsin Madison, Chemical and Biological Engineering

COMMUNICATION

Identifying hydroxylated copper dimers in SSZ-13 via UV-vis-NIR spectroscopy

Received 00th January 20xx,
Accepted 00th January 20xx

DOI: 10.1039/x0xx00000x

Florian Göltl*[a], Saurabh Bhandari[b], Edgard A. Lebrón-Rodríguez[b], Jake I. Gold[b], Stacey I. Zones[c], Ive Hermans[bd], James A. Dumesic[b], Manos Mavrikakis*[b]

Cu-exchanged zeolites are promising materials for the selective conversion of methane to methanol. Their activity is attributed to the presence of small Cu-oxo and Cu-hydroxy clusters, but the nature of active centers in various zeolite structures is still under debate. In this contribution, we combine time dependent density functional theory with spin-orbit coupling to predict the optical spectra of various Cu monomers and dimers in SSZ-13. We furthermore compare theoretical results to experimental measurements and find that the presence of Cu-hydroxy dimers and Cu monomers could potentially explain the experimentally observed UV-vis-NIR spectra.

Natural gas is often an unwanted by-product during crude oil production, which is practiced in remote locations. Methane, the main component of natural gas, is a potent greenhouse gas and very difficult to transport. For these reasons, natural gas is often flared at the extraction site. Converting methane into an easier to transport commodity chemical would be economically and environmentally desirable. At the industrial scale, the chemical conversion of methane follows a two-step process[1], where methane is first converted into synthesis gas and then converted into higher value products such as long chain alkanes[2] or methanol[3]. However, this two-step process requires harsh reaction conditions and is only feasible at large scale, requiring a high capital cost, which renders its application in remote extraction sites impossible. Therefore, research has recently focused on identifying methods that can be applied at remote methane production sites and at a small scale. One promising solution, that has received significant attention, is the stepwise conversion of methane to methanol over Cu- and Fe-exchanged zeolites[4–13]. In this process, a transition metal exchanged zeolite is first activated in an oxidizing atmosphere at high temperatures, subsequently methane is converted to surface bound methoxy species and finally methanol is extracted using water[14,15].

A key question in the conversion of methane to methanol relates to the nature of the active center(s) when the reaction is taking place (*in situ*). For Cu-exchanged zeolites, a variety of different active centers have been proposed, which include Cu-oxo dimers[5,7,15–20], hydroxylated Cu dimers[19,21], hydroxylated Cu monomers[22], as well as Cu-oxo trimers[6]. Recently, we performed a detailed thermodynamic analysis and demonstrated that for Cu-exchanged SSZ-13 (Cu-SSZ-13) activated in an O_2 atmosphere, hydroxylated Cu dimers would be exclusively preferred[14]. The thermodynamically most stable sites during materials activation in an O_2 atmosphere and in the methane to methanol conversion step for different dimer anchoring sites from this study are shown in Figure 1. This theoretical prediction was surprising, especially since the

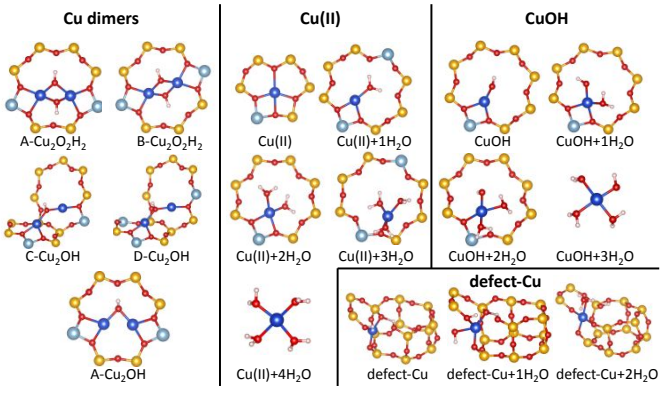

Figure 1: *All Cu exchanged SSZ-13 sites included in our analysis of UV-vis-NIR spectra. We focus on the most stable dimer structures in SSZ-13 for four different Al configuration during activation and reaction conditions[14], as well as divalent Cu monomers, which are either anchored to two Al atoms in close proximity (e.g., Cu(II), only Al atoms in the same ring are displayed)[33] or at a silanol defect (e.g., defect-Cu)[23]. Additionally, Cu-hydroxyl species anchored to one Al atom (CuOH)[33]. In atomistic representations, Si is shown as yellow, O as red, H as white, Al as grey, and Cu as blue, respectively*

[a] *The University of Arizona, Department of Biosystems Engineering, 1177, E 4th St., 85719, Tucson, AZ, United States.*
[b] *The University of Wisconsin – Madison, Department of Chemical and Biological Engineering, 1415 Engineering Drive, 53706 Madison, WI, United States.*
[c] *Chevron Energy Technology Company, Richmond, CA, 94804, United States*
[d] *The University of Wisconsin – Madison, Department of Chemistry, 1101 University Avenue, 53706 Madison, WI, United States*
[e] *Footnotes relating to the title and/or authors should appear here.*
Electronic Supplementary Information (ESI) available: Information about the computational and experimental methods, comparison of spectra calculated with and without spin-orbit coupling and molecular dynamics simulations, as well as calculated spectra for Cu monomers as well as different Cu-oxo and Cu-hydroxy dimers.See DOI: 10.1039/x0xx00000x

presence of hydroxylated Cu dimers in SSZ-13 had never been confirmed experimentally before or proposed as an active center.

One method that can provide detailed information about Cu sites present in zeolites is UV-vis-NIR spectroscopy. At an experimental level, spectral intensities vary between different zeolite materials and different materials pre-treatment methods[17]. However, making unambiguous assignments with respect to the observed spectra is challenging, since static DFT calculations, the most commonly applied methodology in electronic structure calculations, are in principle unable to predict excited states correctly. Only most recently, calculations based on time-dependent density functional theory calculations have been able to reproduce spectral features of monovalent Cu monomers in SSZ-13 with errors in wavenumbers for peak positions that were smaller than 1%[23]. Interestingly, assignments for Cu-SSZ-13 after activation in an O_2 atmosphere using the same methodology were not possible, which was attributed to the potential presence of many different active sites, which leads to overlapping spectroscopic signals[21]. However, the knowledge about the thermodynamically preferred Cu structures in SSZ-13 under various conditions, as presented in our recent study, would help with assigning experimentally observed spectroscopic signals to theoretically calculated spectra[24].

In this contribution we combine time-dependent density functional theoretical calculations, including spin-orbit coupling, and experimental measurements to characterize the Cu sites present in SSZ-13 after activation in O_2 via UV-vis-NIR spectroscopy. We measure UV-vis-NIR spectra for Cu-SSZ-13 after activation in O_2 and compare the results to theoretically predicted spectra for the most stable Cu sites in SSZ-13 and several Cu monomers.

In a first step, we synthesized SSZ-13 with an Si/Al ratio of 14.7 following a synthesis protocol that minimizes Al pairing[25]. This approach ensures separation of Al atoms, which in turn reduces the complexity of the encountered Cu distribution and facilitates the spectroscopic assignment of the encountered species. All details regarding the experimental protocols are given in Supporting Information, section S.1.2. Cu was introduced to this sample using liquid phase ion exchange of $Cu(NO_3)_2$ and we obtained a sample with a Cu/Al ratio of 0.41. Subsequently this sample was activated at 450 °C in an O_2 atmosphere for 8 hours and after removing the sample from the furnace, UV-vis-NIR spectra were measured at room temperature in a glove box atmosphere (<1ppm H_2O, O_2). The resulting spectrum after applying the Kubelka-Munk correction is displayed in Figure 2. We find a broad signal in the low wavenumber region (i.e., wavenumbers between 10000 cm^{-1} and 25000 cm^{-1}) with the highest intensity peak at 13400 cm^{-1} and shoulders at 11500 cm^{-1}, 16230 cm^{-1}, 20000 cm^{-1}, and 21600 cm^{-1} (ordered from highest to lowest intensity). Additionally, a high intensity peak with a maximum at 41000 cm^{-1} is present. The peak positions agree well with data in the literature for similar materials after similar pretreatment routines[7,21,26], even though for our material the intensity of signals in the low wavenumber region is lower.

To identify the sites that lead to the spectroscopic signals observed in experimental measurements we turned to

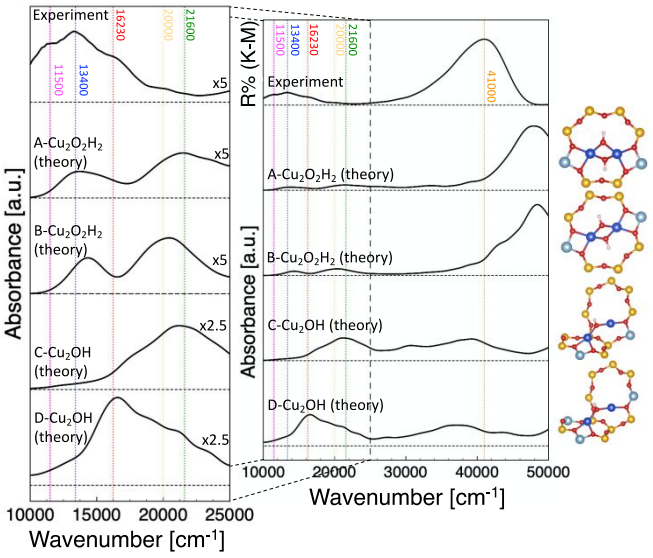

Figure 2: *Experimentally measured UV vis spectra, and theoretically predicted optical spectra for the most stable dimers (A-Cu2O2H2, B-Cu2O2H2, C-Cu2OH, D-Cu2OH) in Cu-SSZ-13 between 10000 cm-1 and 25000 cm-1 (left panel) and 10000 cm-1 and 50000 cm-1(right). Spectra are shown as solid black lines and the zero-intensity line for each spectrum is shown as a horizontal dashed black line. Experimentally observed peaks and shoulders are marked with dashed, vertical lines in various colors. For better visibility, spectra in the left panel have been multiplied by the factor indicated in the respective legend. Colors in atomistic pictures on the right correspond to Figure 1. Theoretically predicted spectra are reported as absorption, experimentally measured spectra are reported as reflectance R% after applying the Kubelka-Munk correction.*

theoretical modeling. In the past, time dependent density functional theory has been shown to be particularly successful in predicting UV-vis-NIR spectra of Cu sites in zeolites[21,23,27]. We perform calculations based on an approach that was successful in modeling spectra of monovalent Cu centers in SSZ-13[23]. Here, a time-dependent hybrid functional with 40% exact exchange is used to predict spectra for a large number of structural snapshots obtained from an MD simulation for a single active site (see Supporting Information section S1.1 for additional details). Spectra for all structural snapshots are then averaged to give the overall spectroscopic signature of the corresponding Cu site. It has furthermore been shown that the inclusion of spin-orbit coupling is crucial to accurately capture potential singlet-triplet transitions in photoluminescence of Cu centers[23]. We therefore also include spin-orbit coupling in the calculation of optical spectra. An analysis for the A-Cu_2OH site in the Supporting Information, Figure S2 shows that both, averaging spectra over a series of structural snapshots and including spin-orbit coupling, significantly modify the obtained spectra. Further analysis in the Supporting Information, section S2 reveals that changes in spectra upon inclusion of spin-orbit coupling are most likely due to the correct capture of singlet-triplet transitions and that similar trends are observed in static calculations for all studied hydroxylated dimers and the CuOH site. All our calculations are carried out in the primitive, rhombohedral unit cell of SSZ-13[28] using periodic boundary conditions as implemented in VASP[29,30], version 5.4.1. Computational details are given in Supporting Information, section S1.1.

As a next step, we apply the proposed methodology to model optical spectra for the hydroxylated Cu dimers that were predicted to be most stable in SSZ-13 after activation in an O_2 atmosphere[14] (structures in Figure 1) with the corresponding spectroscopic signals in Figure 2 and Figure S5. Overlap in spectroscopic signals from different Cu sites makes quantitative assignments based on peak intensity difficult. On top of that, it has been discussed in the literature that the Kubelka-Munk correction applied to the experimentally measured spectra of Cu-exchanged zeolites influences relative intensities of different peak positions[31]. Additionally, superposition of different signals might lead to shifts in peak positions of up to 500 cm^{-1}. In our assignments, we will therefore focus on the main peak positions and will only consider differences in intensities of about one order of magnitude or more as significant.

Indeed, we find that all sites show signals in the low wavenumber range. More specifically, $Cu_2O_2H_2$ sites show signals around 13400 cm^{-1} and 20000 cm^{-1} (B-$Cu_2O_2H_2$) or 13400 cm^{-1} and 21600 cm^{-1} (A-$Cu_2O_2H_2$), while Cu_2OH sites either show signals at 21600 cm^{-1} (C-Cu_2OH) or 16230 cm^{-1} (D-Cu_2OH). While some of the sites show broad background signals at higher wavenumbers, the major peaks lie close to 50000 cm^{-1}, which is outside the illumination range of the experimentally used lamp. These spectroscopic signals indicate that hydroxylated dimers are potentially present in the material, even though the sites show overlapping spectroscopic signals, which makes a clear assignment based on UV-vis-NIR spectroscopy alone impossible. Only the presence of C-Cu_2OH seems unlikely, since it shows a strong signal at 21600 cm^{-1} (note the 2.5x zoom on this spectrum in the left panel of Figure 2), whereas only a low intensity shoulder at this wavenumber is observed in experiment. Additionally, we studied the spectrum for A-Cu_2OH (the spectrum is shown in the Supporting Information, Figure S5), a site predicted to be stable under activation conditions, but unstable at lower temperatures[14]. We find that this site shows signals at 20000 cm^{-1} and 16230 cm^{-1}, but also shows a significant peak around 31520 cm^{-1}. Since such a peak is not observed experimentally, the presence of A-Cu_2OH in Cu-SSZ-13 using our synthesis and activation protocols is unlikely.

The analysis of spectra for the dimer structures reveals that four of the five signals in the low wavenumber range can be assigned to the presence of hydroxylated dimers. Only the signals at 11500 cm^{-1} and 41000 cm^{-1} could not be assigned so far. It is conceivable that these signals originate from Cu monomers that are also present in the material. In the material synthesis we adapted a Na-free approach that has been reported to minimize Al pairing in six-rings of the SSZ-13 framework[25,32]. We therefore focus on two different potential site types present in SSZ-13, namely Cu bound in a unit cell, where Al atoms are close, but not paired in the same six-member ring, and CuOH, which represents the limiting case of well separated Al atoms[33]. Both Cu sites are shown in Figure 1. Phase diagrams indicate that CuOH and Cu should be present without a water coordination shell during activation. However, exposure to a glove box environment might lead to water adsorption to Cu monomers. For these sites, we therefore explore scenarios where they are coordinated to up to four (Cu(II)) or three (CuOH) water molecules and the calculated spectra are shown in Figure 3, Figure S5 (Cu(II)+1H_2O, Cu(II)+2H_2O, Cu(II)+4H_2O), and Figure S6 (CuOH+1H_2O and CuOH+3H_2O). It is immediately apparent that the presence of CuOH and Cu(II) sites that are not coordinated to H_2O molecules is unlikely, since CuOH shows a very distinct peak around 36890 cm^{-1} and Cu leads to a broad signal above 20000 cm^{-1}, which are both not observed in experiments. CuOH coordinated to H_2O molecules shows a weak signal around 15000 cm^{-1} (the exact position depends on the H_2O coordination) and an additional signal centered around 41000 cm^{-1}. Cu sites coordinated to H_2O also show weak low wavenumber transitions and either a broad signal between 25000 cm^{-1} and 45000 cm^{-1} for Cu coordinated to one H_2O or a broad signal with highest intensities above 40000 cm^{-1}. Even though the exact water coordination of the different sites is unknown, in particular the presence of CuOH coordinated to one or two water molecules would explain the presence of the experimentally observed peak at 41000 cm^{-1} and would also contribute signals in the low wavenumber range. At the same time the presence of other Cu monomers as minority species cannot be excluded. However, most signals in the low wavenumber region for Cu monomers are low in intensity and also none of the Cu dimer sites considered here can explain the presence of the 11500 cm^{-1} peak.

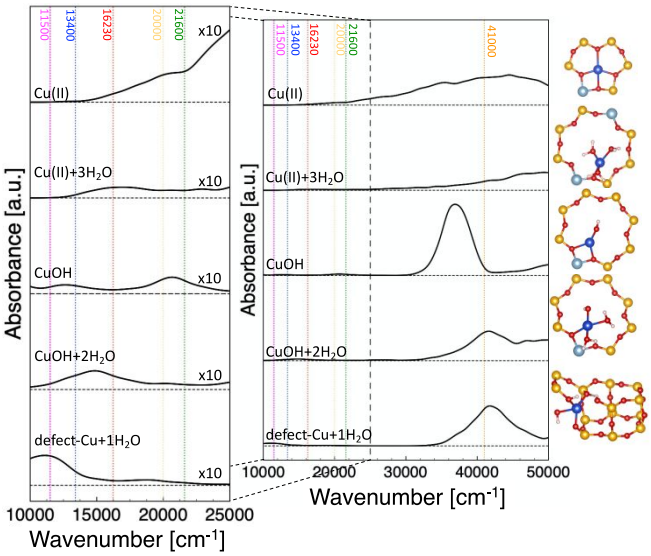

Figure 3: *Theoretically predicted optical spectra for different Cu monomers in Cu-SSZ-13 between 10000 cm^{-1} and 25000 cm^{-1} (left panel) and between 10000 cm^{-1} and 50000 cm^{-1}(right) . Spectra are shown as solid black lines and the zero-intensity line for each spectrum is shown as a horizontal dashed black line. Experimentally observed peaks and shoulders are marked with dashed, vertical lines in various colors for readability. For better visibility, spectra in the left panel have been multiplied by the factor indicated by each spectrum. Colors in atomistic pictures on the right correspond to Figure 1.*

To understand the origin of the 11500 cm^{-1} signal, we furthermore studied divalent Cu sites anchored in a silanol defect (defect-Cu shown in Figure 1) with up to two water molecules adsorbed and the resulting spectra are shown in Figure 3 and Figure S6 in the Supporting Information. Indeed, we find that all three water coordination environments show a major signal around 41000 cm^{-1} with an additional signal at either 11500 cm^{-1} for Cu coordinated to one H_2O molecule or around 10000 cm^{-1} in the other two cases.

These results show that a mixture of different sites is present after activation in O_2 because no one site can reproduce all the peaks observed. We find that several hydroxylated Cu dimers are present in the material, which contribute to spectroscopic signals at 13400 cm^{-1}, 16230 cm^{-1}, 20000 cm^{-1}, and 21600 cm^{-1}. Furthermore, CuOH coordinated to either one or two H_2O molecules contributes to a major peak at 41000 cm^{-1}. These assignments agree well with phase diagrams published in previous work[14], which predict the stabilization of hydroxylated Cu dimers after activation in O_2, as long as the respective anchoring points for these sites are available. The only site modeled in this contribution that agrees with the experimentally measured peak at 11500 cm^{-1} is a divalent Cu atom bound to a silanol defect and one H_2O molecule. Additionally, this site contributes to the experimentally observed peak at 41000 cm^{-1}. The presence of such a defect-anchored Cu site has not been suggested before and could either be attributed to silanol defects present in our material or to other Cu sites bound at the surface or at grain boundaries of the zeolite particle, where a Cu atom encounters a bonding environment similar to framework defects. More specifically, defect-anchored Cu shows similarities to Cu atoms supported on alumina[34], which have been shown to convert methane to methanol. We therefore hypothesize that these sites might not be innocent in the conversion of methane to methanol.

In the past, Li et al. also modeled the UV-vis-NIR spectra of Cu sites in SSZ-13 using time dependent DFT[21]. In their analysis they concluded that the spectra resulted from the superposition of various spectroscopic signals from different sites, but an unambiguous assignment based on their results was not possible due to the complexity of the encountered site distribution. However, their study focused only on a limited number of Cu sites and did not include spin orbit coupling, which we have shown to be crucial to arrive at quantitatively accurate peak positions (see Supporting Information section S2).

In the experimental literature, the same UV-vis-NIR signals have mainly been attributed to the presence of different Cu monomers, CuOH, or Cu-oxo sites[7,17,31]. More specifically, different Cu-oxo dimers (Cu_2O, Cu_2O_2) have been suggested to be present in the material and show spectroscopic signals in the low wavenumber range (10000 cm^{-1} – 25000 cm^{-1}). To understand whether these species can lead to the experimentally observed peaks, we modeled their spectra, which are shown in the supporting information Figure S7 and Figure S8. Indeed, no Cu_2O and Cu_2O_2 site shows the experimentally observed signal at 16230 cm^{-1}. Additionally, all studied Cu-oxo dimers lead to strong spectral intensities between 20000 cm^{-1} and 40000 cm^{-1}, which are not observed in our experimental measurements, even though they have been observed for Cu-SSZ-13 samples obtained from different synthesis and/or pretreatment protocols[26,31]. Hence, we conclude that Cu-oxo dimers are at best a minority species following the synthesis and materials preparation protocols applied here.

Interestingly, we find that the signal intensity in the wavenumber range between 10000 cm^{-1} and 25000 cm^{-1} in our experimental measurements is lower compared to reports in the literature[7,17,21,26]. This indicates that in the material we synthesized fewer Cu dimer sites, which contribute to these signals, are formed compared to measurements in the literature[7,17,21,26]. This observation holds true, even though we chose a synthesis route that reduces the number of Cu monomers anchored in six-member rings with Al pairs that are thermodynamically more stable than dimers during catalyst activation. If the presence of specific Cu monomers in SSZ-13 was the only mechanism that reduces dimer formation during catalyst activation, a larger number of Cu dimers should be present in materials obtained from our synthesis approach. However, this is not the case, and a possible explanation is that the change in synthesis approach does not only modify the Al pairings in six-member rings but might lead to a change in availability of dimer exchange sites. Alternatively, the distance distribution between Al atoms in materials obtained from our synthesis approach might be skewed towards larger Al-Al distances, which would only allow for the formation of a smaller number of dimers during activation[35].

Conclusions

In this contribution we studied the UV-vis-NIR spectrum of Cu-exchanged SSZ-13 after activation in an O2 atmosphere. We calculated optical spectra for the most stable sites in Cu-SSZ-13 using time dependent density functional theory in combination with spin orbit coupling and compared our results to experimentally measured spectra of Cu-SSZ-13 after activation in an O2 atmosphere. We found that a combination of spectroscopic signals caused by hydroxylated Cu dimers and extraframework and defect bound Cu monomers can explain all observed spectroscopic signals. Additionally, signals of Cu-oxo dimers[7,17], which have been previously suggested to be present in Cu-SSZ-13, are absent in experimental spectra.

These results make the presence of hydroxylated Cu dimers in SSZ-13 after activation in O_2 following the synthesis and preparation protocol applied in this work highly likely, which agrees with theoretically calculated phase diagrams presented in the literature[14]. In the future it will be interesting to see how we can use these insights to better understand the ability of Cu-SSZ-13 in particular and Cu-exchanged zeolites in general to convert methane to methanol.

Acknowledgements

This work was supported by the National Science Foundation, grant number CHE-1800284. We acknowledge computational time at the National Energy Research Scientific Computing Center (NERSC), a DOE Office of Science User Facility supported by the Office of Science of the U.S. Department of Energy, contract DE-AC02-05CH11231.

Conflicts of interest

There are no conflicts to declare.

Notes and references

[1] H. T. Luk, C. Mondelli, D. C. Ferré, J. A. Stewart, J. Pérez-

Ramírez, *Chem. Soc. Rev.* **2017**, *46*, 1358–1426.
[2] H. Jahangiri, J. Bennett, P. Mahjoubi, K. Wilson, S. Gu, *Catal. Sci. Technol.* **2014**, *4*, 2210–2229.
[3] L. C. Grabow, M. Mavrikakis, *ACS Catal.* **2011**, *1*, 365–384.
[4] M. Ravi, V. L. Sushkevich, A. J. Knorpp, M. A. Newton, D. Palagin, A. B. Pinar, M. Ranocchiari, J. A. Van Bokhoven, *Nat. Catal.* **2019**, *2*, 485–494.
[5] M. H. Groothaert, P. J. Smeets, B. F. Sels, P. A. Jacobs, R. A. Schoonheydt, *J. Am. Chem. Soc.* **2005**, *127*, 1394–1395.
[6] S. Grundner, M. A. C. Markovits, G. Li, M. Tromp, E. A. Pidko, E. J. M. Hensen, A. Jentys, M. Sanchez-Sanchez, J. A. Lercher, *Nat. Commun.* **2015**, *6*, 7546.
[7] B. Ipek, M. J. Wulfers, H. Kim, F. Göltl, I. Hermans, J. P. Smith, K. S. Booksh, C. M. Brown, R. F. Lobo, *ACS Catal.* **2017**, *7*, 4291–4303.
[8] V. L. Sushkevich, D. Palagin, M. Ranocchiari, J. A. Van Bokhoven, *Science (80-.).* **2017**, *356*, 523–527.
[9] B. E. R. Snyder, M. L. Bols, R. A. Schoonheydt, B. F. Sels, E. I. Solomon, *Chmical Rev.* **2018**, *118*, 2718–2768.
[10] B. E. R. Snyder, P. Vanelderen, M. L. Bols, S. D. Hallaert, L. H. Böttger, L. Ungur, K. Pierloot, R. A. Schoonheydt, B. F. Sels, E. I. Solomon, *Nat. Publ. Gr.* **2016**, *536*, 317–321.
[11] B. E. R. Snyder, M. L. Bols, H. M. Rhoda, D. Plessers, R. A. Schoonheydt, B. F. Sels, E. I. Solomon, *Science (80-.).* **2021**, *373*, 327–331.
[12] F. Göltl, C. Michel, P. C. Andrikopoulos, A. M. Love, J. Hafner, I. Hermans, P. Sautet, *ACS Catal.* **2016**, *6*, 8404–8409.
[13] K. Narsimhan, K. Iyoki, K. Dinh, Y. Román-Leshkov, *ACS Cent. Sci.* **2016**, *2*, 424–429.
[14] F. Göltl, S. Bhandari, M. Mavrikakis, *ACS Catal.* **2021**, *11*, 7719–7734.
[15] D. K. Pappas, E. Borfecchia, M. Dyballa, I. Pankin, K. A. Lomachenko, A. Martini, M. Signorile, S. Teketel, B. Arstad, G. Berlier, C. Lamberti, S. Bordiga, U. Olsbye, K. P. Lillerud, S. Svelle, P. Beato, *J. Am. Chem. Soc.* **2017**, *139*, 14961–14975.
[16] D. T. Bregante, L. N. Wilcox, C. Liu, C. Paolucci, R. Gounder, D. W. Flaherty, *ACS Catal.* **2021**, *11*, 11873–11884.
[17] H. M. Rhoda, D. Plessers, A. J. Heyer, M. L. Bols, R. A. Schoonheydt, B. F. Sels, E. I. Solomon, *J. Am. Chem. Soc.* **2021**, *143*, 7531–7540.
[18] P. Vanelderen, B. E. R. Snyder, M.-L. Tsai, R. G. Hadt, J. Vancauwenbergh, O. Coussens, R. A. Schoonheydt, B. F. Sels, E. I. Solomon, *J. Am. Chem. Soc.* **2015**, *137*, 6383–6392.
[19] U. Engedahl, H. Grönbeck, A. Hellman, *J. Phys. Chem. C* **2019**, *123*, 26145–26150.
[20] P. Sazama, J. Moravkova, S. Sklenak, A. Vondrova, E. Tabor, G. Sadovska, R. Pilar, *ACS Catal.* **2020**, *10*, 3984–4002.
[21] H. Li, C. Paolucci, I. Khurana, L. N. Wilcox, F. Göltl, J. D. Albarracin-Caballero, A. J. Shih, F. H. Ribeiro, R. Gounder, W. F. Schneider, *Chem. Sci.* **2019**, *10*, 2373–2384.
[22] A. R. Kulkarni, Z. J. Zhao, S. Siahrostami, J. K. Nørskov, F. Studt, *ACS Catal.* **2016**, *6*, 6531–6536.
[23] F. Göltl, S. Conrad, P. Wolf, P. Müller, A. M. Love, S. P. Burt, J. N. Wheeler, R. J. Hamers, K. Hummer, G. Kresse, M. Mavrikakis, I. Hermans, *Chem. Mater.* **2019**, *31*, 9582–9592.
[24] F. Göltl, P. Müller, P. Uchupalanun, P. Sautet, I. Hermans, *Chem. Mater.* **2017**, *29*, 6434–6444.
[25] J. R. Di Iorio, R. Gounder, *Chem. Mater.* **2016**, *28*, 2236–2247.
[26] F. Giordanino, P. N. R. Vennestrøm, L. F. Lundegaard, F. N. Stappen, S. Mossin, P. Beato, S. Bordiga, C. Lamberti, *Dalton Trans.* **2013**, *42*, 12741–61.
[27] O. Adeyiga, O. Suleiman, S. O. Odoh, *Inorg. Chem.* **2021**, *60*, 8489–8499.
[28] F. Göltl, J. Hafner, *J. Chem. Phys.* **2012**, *136*, 064501.
[29] G. Kresse, D. Joubert, *Phys. Rev. B* **1999**, *59*, 1758–1775.
[30] G. Kresse, J. Furthmüller, *Comput. Mater. Sci.* **1996**, *6*, 15–50.
[31] C. Negri, M. Signorile, N. G. Porcaro, E. Borfecchia, G. Berlier, T. V. W. Janssens, S. Bordiga, *Appl. Catal. A Gen.* **2019**, *578*, 1–9.
[32] J. Devos, M. L. Bols, D. Plessers, C. Van Goethem, J. W. Seo, S. J. Hwang, B. F. Sels, M. Dusselier, *Chem. Mater.* **2020**, *32*, 273–285.
[33] F. Göltl, A. M. Love, I. Hermans, *J. Phys. Chem. C* **2017**, *121*, 6160–6169.
[34] J. Meyet, K. Searles, M. A. Newton, M. Wörle, A. P. van Bavel, A. D. Horton, J. A. van Bokhoven, C. Copéret, *Angew. Chemie Int. Ed.* **2019**, *58*, 9841–9845.
[35] C. Paolucci, I. Khurana, A. A. Parekh, S. Li, A. J. Shih, H. Li, J. R. Di Iorio, J. D. Albarracin-caballero, A. Yezerets, J. T. Miller, W. N. Delgass, F. H. Ribeiro, W. F. Schneider, R. Gounder, *Science (80-.).* **2017**, *5630*, 1–11.